Hydrogen at extreme pressures

(**Review Article**)

Alexander F. Goncharov[1,2]

[1]*Geophysical Laboratory, Carnegie Institution of Washington, Washington, D.C. 20015, USA*
[2]*Key Laboratory of Materials Physics, Institute of Solid State Physics, Chinese Academy of Sciences,*
Hefei 230031, China
E-mail: agoncharov@ciw.edu

Ross T. Howie and Eugene Gregoryanz

Centre for Science at Extreme Conditions and School of Physic and Astronomy, University of Edinburgh, Mayfield
Road, Edinburgh EH9 3JZ, United Kingdom

Here we review recent experimental and theoretical studies of hydrogen approaching metallization regime. Experimental techniques have made great advances over the last several years making it possible to reach previously unachievable conditions of pressure and temperature and to probe hydrogen at these conditions. Theoretical methods have also greatly improved; exemplified through the prediction of new structural and ordered quantum states. Recently, a new solid phase of hydrogen, phase IV, has been discovered in a high-pressure high-temperature domain. This phase is quite unusual structurally and chemically as it represents an intermediate state between common molecular and monatomic configurations. Moreover, it shows remarkable fluxional characteristics related to its quantum nature, which makes it unique among the solid phases, even of light elements. However, phase IV shows the presence of a band gap and exhibits distinct phonon and libron characteristic of classical solids. The quantum behavior of hydrogen in the limit of very high pressure remains an open question. Prospects of studying hydrogen at more extreme conditions by static and combined static-dynamic methods are also presented.

Contents

1. Introduction

Hydrogen has a special interest for many fields of research as it represents the perfect model object due to its seeming simplicity and abundance in the cosmos [1–4]. One of the objectives of studying hydrogen at extreme pressures is to rationalize the notion of metallic hydrogen as a future energy carrier. There are three major technical drivers in this pursuit: theoretical calculations and dynamic and static compressions. Each has its own pressure — temperature — time-scale domain, which largely do not intersect and this poses a serious difficulty in unifying and comparing results. This issue is now being addressed by improving and modifying these techniques and by creating new combined static-dynamic experimental methods.

With regard to theoretical and dynamic experimental studies, we refer readers to the recent review on mainly the theoretical approach to study hydrogen under extreme conditions [5], which also contains a brief review of experimental works. Study of hydrogen using dynamic compression (see the review papers [1,6,7]) is progressing very rapidly now with a development of laser driven technique compression of statically pre-compressed samples [8,9].

The purpose of this review is to critically look at the experimental studies of the past two decades, which have been performed using diamond anvil cell (DAC) techniques and combined DAC heating experiments, covering all known solid phases of hydrogen and its melting curve.

Static compression of hydrogen to very high pressure is technically very challenging. Hydrogen is very compressible, while the materials commonly used to form the sample chamber around it are not. Generating high-pressure on hydrogen requires larger compression of the gasket material than with less compressible samples due to the limitation of plastic flow. Secondly, hydrogen is very diffusive; it tends to penetrate and rupture any small crack in both the diamond and gasket. In the case of diamond this always results in premature anvil failures. These effects accelerate with temperature: rarely occurring below 100 K, but increasing substantially above 200 K. Owing to this, until 2011, there were no reliable reports on static compression of hydrogen or deuterium above 180 GPa at room temperature [10]. Improved sample loading techniques, which include diamond protective coating, focused electron beam (FIB) gasket drilling, and better optimized anvil geometry have recently allowed achieving static compression of hydrogen well above 300 GPa at 300 K [11].

These technical breakthroughs resulted in extending the achievable pressure range for hydrogen research up to 320 GPa at 300 K [11] and up to 360 GPa at 80 K [12]. New semiconducting (or semimetallic) solid phase hydrogen has been discovered above 220 GPa at 300 K by combined experimental (Raman and optical spectroscopy) and theoretical efforts [11,13]. A conflicting report claiming electrically conducting hydrogen in the fluid state above 260–270 GPa has been earlier published by Eremets and Troyan [14] infrared measurements in phase III to 360 GPa [12] also did not report metallic conductivity. However, one should note, that pressure metrology remains a problem as measurements of the diamond Raman edge as pressure calibrant [15] are somewhat uncertain, and, moreover, some experiments relied on higher pressure extrapolations [12]. Here, we will review the recent works and present prospects of new technical advances, which can enable next major breakthroughs.

2. Phase relations

Until recently, only three solid states of hydrogen have been known (Fig. 1). Phase I is a plastic phase of freely rotating molecules forming an hcp lattice whilst phases II and III are partially (or completely) ordered phases, which appear at lower temperatures and/or higher pressures (see Refs. 2, 16, 17 for review). The symmetries and orientation order types of phases II and III have been extensively discussed in the literature based on experimental spectroscopy observations [2,16,17,19,33–37] and theoretical calculations [20,38–45], however the available x-ray diffraction data are still not conclusive [46–48]. The important issue of ortho–para dis-
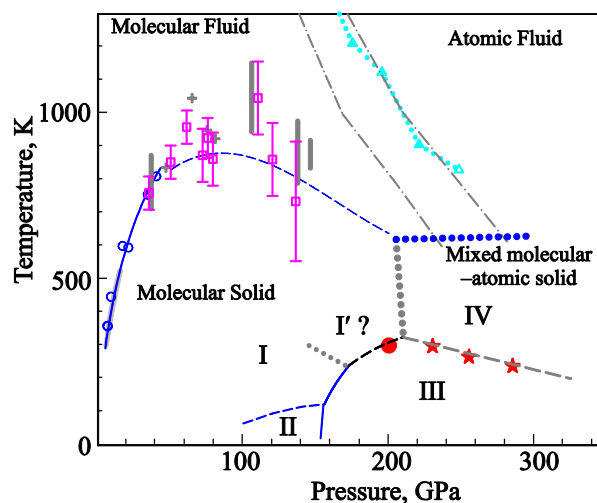

Fig. 1. (Color online) Phase diagram of hydrogen. The I–II and I–III phase line for normal H_2 are from Ref. 18; the I–III phase (solid line) has been corrected as proposed in Ref. 17. The filed circle is room temperature data from Ref. 11; the dashed line is the proposed I–III phase line at high *T*. The dotted gray line shows a schematic location of the I–I' phase line inferred in Refs. 19–23. The melting measurements are from Refs. 24–29: thick gray line (Ref. 24), open circles (Ref. 25), crosses (Ref. 27), vertical gray bars (Ref. 28), open squares (Ref. 26), dashed line (Ref. 29). Stars correspond to the III–IV transition [11] (see also Ref. 30). Open triangles and gray dashed-dotted lines (from DFT and QMC calculations) are theoretical results for a liquid-liquid transition [31,32] associated with the molecular dissociation. Thick dotted gray and blue lines are suggested I–IV and IV–liquid lines, respectively.

tinction, and its effect on both the structure and phase transitions, has also been discussed extensively. The available data remain fragmentary due to difficulties in performing experiments on materials with pure ortho–para composition. Nonetheless, the current consensus is that the ortho–para distinction does not affect the transition to phase III, which is suggested to be classically orientationally ordered [18,49]. Due to technical difficulties, the extension of the phase line between phases I and III to room temperature could not have been reached until recently. It has been proposed [23] based on the crystal symmetry arguments that this line should have a termination at a critical point with finite *P–T* conditions, and phase I', with the same symmetry as phase III, merges with phase I in the triple point, giving rise to the I–I' phase line (Fig. 1). Nevertheless, suggestions about the existence of phase I' based on these symmetry considerations, theoretical calculations [20] or experimental observations of subtle changes in vibrational frequencies [21] have yet to be confirmed (see Ref. 17 for more information). Instead, recently it has been found that the I–III phase line does extend to room temperature, and perhaps even beyond, where it meets a new phase line with solid phase IV (Fig. 1). At room temperature the transition sequence is I–III–IV, and the corresponding transitions occur at 200 and 230 GPa (in H_2) [11].

3. Melting and fluid behavior

Determination of the melting line of hydrogen, especially in the limit of high pressures, remains one of the most challenging experimental tasks. Theoretical two-phase simulations up to 200 GPa suggest that there is a decline in the melting temperature above 90 GPa related to softening of the intermolecular interactions, which occur at a faster rate in the liquid than in the solid as a function of pressure [29]. First principles calculations performed on this and other works also suggest the presence of another high-temperature boundary above the melt line related to the molecular dissociation. This transformation is often called the plasma line but can be also considered as a first-order liquid-liquid transition [32,50–53]. Extrapolations of the melt line and the liquid–liquid phase transition [29] determined in theoretical calculations suggest the presence of a triple point at 300 GPa and 400 K. Above this pressure, the solid is expected to melt into a metallic liquid.

Two major experimental techniques have been used to detect melting: visual observations, which include detection of the laser speckle pattern [24,27,28], and Raman spectroscopy measurements [25,26]. Generally, the results of visual observations should be considered quite reliable at relatively low pressures as the optical contrast between solid and fluid is sufficiently large due to the difference in the refractive indices. The results of two available experimental studies [24,54] are in agreement within the *P–T* range of overlap. The study by Datchi *et al*. [24] extended the melting line up 15.2 GPa and 530 K, but experienced difficulties in reaching more extreme conditions because the metallic gasket materials used could not contain the hydrogen sample. These visual observation experiments required substantial time as very slow temperature change is required to stabilize fluid and solid materials in equilibrium. Gregoryanz *et al*. [25] used cubic boron nitride and alumina insets in rhenium gaskets and employed express Raman observations to detect melting. At melting, they observed a small Raman vibron discontinuity up to 44 GPa, but no further discontinuities have been detected above this pressure. They also reported a large increase in the negative temperature shift of the Raman vibron with pressure. Combined melting temperature data to 44 GPa obtained in resistive heating experiments [24,25,54] suggest a possible melting line maximum near 100 GPa and 1000 K in qualitative agreement with the theoretical calculations of Ref. 29.

Experiments on the melting of hydrogen to higher pressures have been performed using laser heating techniques [26–28] including pulsed laser heating. The results of these very challenging experiments remain largely controversial, as there are a number of inconsistent observations. In particular the results of Deemyad, and Silvera [27], which utilized visual observations, are standing alone, as they suggest a very narrow maximum at the melting line, inconsistent

with the theoretical predictions and the results of other measurements. Notably, Deemyad, and Silvera have reported four pressure points obtained in one single experimental run; they have not been able to provide any experimental evidence of presence of hydrogen in the high-pressure cavity after the initial laser heating experiments. The results of this study were not reproduced in subsequent investigations [26,28], which presents results of multiple loads, and clear Raman evidence of hydrogen present in the sample cavity. Both studies [26,28] suggest that the melt line has a broad maximum near 100 GPa, in a qualitative agreement with the theoretical calculations of Ref. 29. However, the diagnostics of melting in Refs. 26, 28 is somewhat controversial. Eremets and Trojan [28] report changes in the laser speckle pattern and a large reversible drop in resistivity of a Pt foil which probe the sample cavity. These observations may be related to melting but could, in principle, be due to chemical reactions, or other phenomena unrelated to melting. A drop in the resistance of the Pt foil, claimed by Eremets and Trojan to be an indication of melting, was proposed by them to be due to a shunting by conducting fluid hydrogen. Instead, we suggest that the thermal flux, out of the laser heated Pt foil, increases rapidly through the convection in molten hydrogen, causing the foil to drop the temperature, and hence the electrical resistance. Subramanian *et al*. [26] reported on a large discontinuity of the Raman vibron at melting and attributed this to a change in chemical bonding in fluid hydrogen. However, this observation seemingly contradicts Raman measurements in resistively heated DACs, where a very small, or even no discontinuity was observed [25]. The reason for such discrepancy may be due to difficulties of containing, and hence measuring Raman spectra of fluid hydrogen in resistively heated DACs. Alternatively very large temperature gradients across the sample can give rise to bimodal Raman spectra observed in the laser heating experiments [26] as the Raman vibron shows a very steep temperature dependence. The available experimental melting data of hydrogen provide definitive prove of a maximum in the melting line.

Conventionally, it is assumed that fluid hydrogen is molecular at moderate pressures below the triple point with solid and dissociated fluid > 200 GPa, < 1000 K. Raman measurements of fluid hydrogen [26,55] however show a continuous change with pressure in intramolecular bonding in the fluid state. Goncharov and Crowhurst [55] also found a large increase in the vibron bandwidth accompanied by a decreased vibron anharmonicity deduced from the spacings between excited vibrational states. Subramanian *et al*. [26] show that the roton modes essentially disappear in the fluid state above 30 GPa. These observations can be understood due to the drastic decrease in lifetime of molecular states in fluid hydrogen with pressure. The lifetime of the molecular states become comparable with the vibrational period, but are shorter than the rotational period, making the latter unobservable.

Until recently, experimental observations of conducting states in dense hydrogen could only be performed in shock wave experiments [56–59] and static DAC experiments on hydrogen exceeding temperatures of 3000 K were inaccessible. Recently, Goncharov *et al.* [60] developed a new optical spectroscopy technique in pulsed laser heated DAC which allow to measure optical spectra in the visible spectral range. The sample is heated by 1–5 μs pulses of electrically modulated Yb fiber laser at 1070 nm. The optical spectra are measured using a supercontinuum generated in a photonic crystal fiber and are recorded as a function of time using a streak camera in a single two-dimensional CCD image along with the radiation spectra to measure the temperature spectroradiometrically. Such technique has opened a window of opportunity to probe hot dense hydrogen at *P–T* conditions thought to be unachievable through static compressions.

4. Phase II

The transition to phase II has been originally described as the one from spherically symmetric rotational states of pure para H_2 or ortho D_2 to a broken symmetry phase in which these symmetric states deform and material transforms an orientationally ordered state [34]. It has been shown that mixed ortho-para materials (for example with a normal composition corresponding to the high-*T* limit [61]) also transform to phase II (which reveals different rotational dynamics [37] and perhaps even a different crystal symmetry) at lower pressures. A very large isotope effect has been observed for the transition to phase II [34,62,63]. The large isotope effect on the transition pressure to BSP phase suggests that the transition is related to ordering of the quantum rotational degrees of freedom [18,49] as the rotational constants $B = h/4\pi^2 cI$, where I is the rotational moment of inertia, governing the rotational energies are very different for H_2 and D_2. On the microscopic level, at the entry to phase II, free molecular rotations are expected to transform to wide-angle librations for some of the rotational coordinates, which can be largely incoherent [39]. The first-principles path-integral molecular dynamic calculations revealed the quantum character of these molecular motions, however, these experience a "quantum localization" (or "quantum confinement") as molecular rotations become hindered in some rotation directions [38]. In contrast, recent *ab initio* path integral molecular dynamics (PIMD) of Li *et al.* [49] do not support the "quantum confinement" and instead suggest that the transition is governed by a competition between anisotropic inter-molecular interactions, and the thermal and quantum nuclear fluctuations.

Raman spectra of phase II reveal a combination of free molecular rotation excitations and libron like vibrations characteristic of the orientationally ordered molecules [35]. Raman and IR spectra of vibron modes have been used to map the II–I phase line. Below approximately 140 GPa, the

transition can be traced by observing a small vibron discontinuity [16,18,19,34,37]. Above 140 GPa, the vibron frequency has a strong temperature dependence in phase II prior to the transition to phase I [17,33], suggesting that the orientational ordering develops gradually with pressure within phase II.

The determination of the structure of orientationally ordered hydrogen phases is a very challenging topic. Theoretical structure search is difficult because phase II retains a large amount of orientational disorder. Thus, a single theoretical approach (*e.g.*, density functional theory, DFT) does not work well. Recently, Li *et al.* [49] suggested using PIMD technique for the most stable static molecular configuration to account for quantum nuclear motion at finite temperatures. However, the validity of these results needs to be verified against the experimental observations.

The experimental data are also very limited [46–48,64]. Normally, only 1 or 2 of the strongest reflections originating from 100 and 101 major peaks of hcp phase I of hydrogen could be observed. However, Goncharenko and Loubeyre [47] additionally reported one extra reflection observed in single crystal x-ray and neutron diffraction of D_2. They interpreted this as due to an incommensurate long-range order. In contrast, a Raman study [37] suggested 3x5 Brillouin zone folding. Moreover, the modulation appears at a lower pressure than that reported for the I–II transition in Raman measurements [37].

5. Phase III

Phase III has been discovered in Raman observations at 77 K: the Raman vibron revealed an astonishing 100 cm^{-1} discontinuity at 155 GPa, and observations showed a two-phase coexistence in the pressure range of about 20 GPa, which is characteristic of the first-order transition [65]. Subsequent infrared absorption (IR) measurements showed a two order of magnitude increase in the vibron mode activity in phase III [36,66–68]. These observations initiated a number of suggestions about a new chemical bonding type in phase III related to a large intermolecular charge transfer [69]. However, direct reflectivity measurements [68] showed that the dipole moment associated to the IR vibron is very small (0.04e at 210 GPa), so the charge transfer may be of dynamic nature and be restricted within the molecule. However, density functional theory does predict a small structural distortion of the parent hexagonal closed-packed lattice of phase I [39,44].

For a long time vibrational spectroscopy served as the sole source of information on properties of phase III. Raman spectroscopy measurements of phase III revealed a number of observations, which shed light on the structural and dynamical properties of phase III. In addition to the vibron discontinuity, the II–III transition is characterized by a total alteration of the low-frequency spectra: the roton spectra (or their remnants) disappear and a number of new

peaks appear at the transition to phase III (Fig. 2). These show a very strong pressure dependence, which identify them as the lattice modes (translational and librational) unlike the rotational modes (rotons) in phases I and II which are very weakly pressure dependent [34,70]. The frequencies of the Raman modes increase strongly with pressure and the modes become sharper (Fig. 2) [35]. Raman and IR spectra of phase III are also strongly temperature dependent. The Raman and IR vibron frequencies increase with temperature continuously in a wide temperature range which was determined in quasi-isobaric experimental scans [17–19]. There is a discontinuity in the vibron frequency at the II–III and I–III transitions , which quickly decreases with pressure and was reported to disappear above 235 K (in D_2) [37] even though two vibron peaks were observed near the transition. This was interpreted as a (tri)critical point, where either the transition becomes second order or terminates, so there is no distinction between phases I and III at higher pressures (and temperatures). The IR intensity was also found to decrease in intensity in the temperature runs [18,33] similar to that of the Raman and IR frequencies. This was described by a Maier–Saupe model [71], which characterizes the orientational ordering of classical rotors and initially was derived for liquid crystals. Within this model, the IR frequency and intensity and Raman frequency of the vibron can be treated as scalar order parameters characterizing the orientational ordering in phase III [18,33]. The conclusion about the nature of orientational ordering in low-temperature phase III is also supported by a relatively weak isotope effect (cf. transition pressures of transitions to phase II for H_2 and
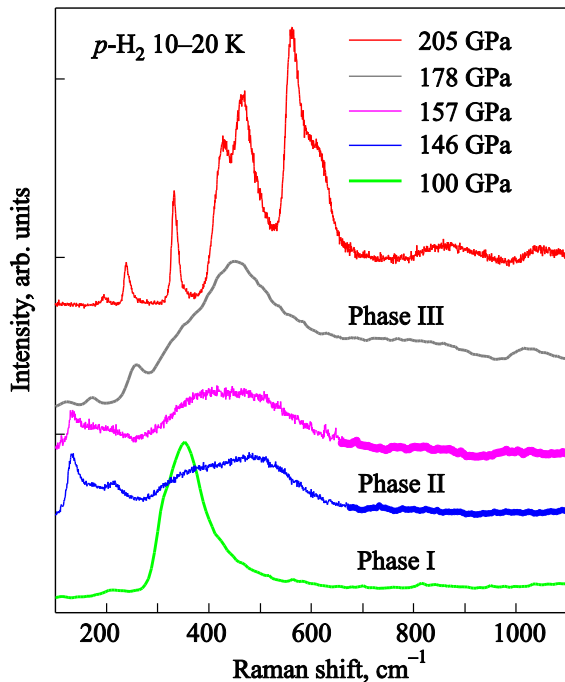
D_2), the insensitivity of the transition pressure to the ortho-para concentration [18,35] and the observation of the total disappearance of the roton Raman bands (Fig. 2).

As in the case of phase II, the determination of the structure of orientationally ordered phase III of hydrogen is a very challenging topic and the experimental data are very limited [46]. Moreover, only 1 or 2 strongest reflections originated from 100 and 101 major peaks of hcp phase I of hydrogen could be observed. Recently, x-ray diffraction studies have been performed in the *P–T* range of stability of phase III (>155 GPa below 120 K) [46]. The results suggest that an hcp lattice remains a structural basis of phase III.

Theoretical structural search for high-pressure phases of hydrogen has a long history [39–44,72–74]. Here we briefly review the most relevant works for the high-pressure (>100 GPa) range, where the effects of quantum rotations and ortho-para distinctions is substantially diminished. In this regime the (DFT) should be well applicable. However, these results should also be treated carefully as the quantum effect related to large zero point energy make substantial contributions into the free energy.

The results of an extensive theoretical DFT structural search [40,42] suggested a monoclinic *C2/c* structure as the primary candidate for phase III. A number of structures are very competitive in enthalpy in the pressure range of interest; the results depend on the level of DFT theory, form of pseudopotentials used, and treatment of proton zero point motion [40]. It is interesting that none of these structures agree well with the x-ray diffraction data (Fig. 3), although some level of agreement has been achieved with the Raman and IR data [35,67,75], especially with the presence of a strong IR vibron absorption mode. It is interesting that hybrid DFT calculations [76] find the *P*6_3/*m* structure

Fig. 2. (Color online) Raman spectra of hydrogen through transitions to phases II and III [35].
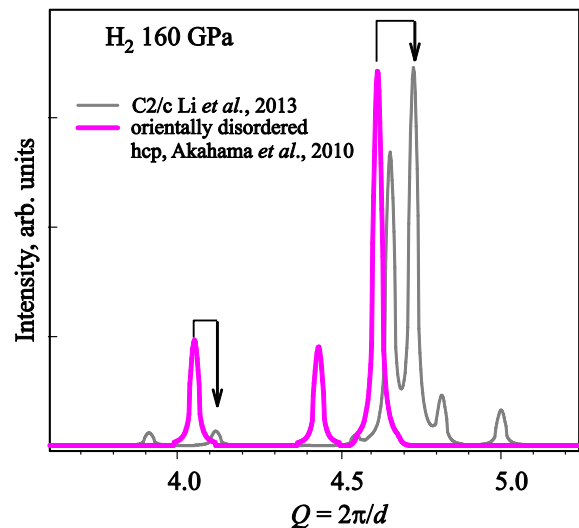

Fig. 3. (Color online) X-ray diffraction of phase III of hydrogen. Gray line: *C2/c* structure from Ref. 49 and pink line is an hcp of molecular centers with the lattice parameters from the experimental study of Akahama *et al.* [46].

(which would yield the x-ray pattern that nicely agrees with the x-ray experiment) the most stable, although the previous study found that this structure is dynamically unstable above 120 GPa [40]. However, this structure seems inconsistent with the IR observations. For the sake of completeness, we would like to mention that the $Cmc2_1$ structure proposed by Toledano *et al.* [23] based on group theory is somewhat higher in DFT enthalpy, although Raman and IR activity and x-ray diffraction patterns broadly agree with the observations.

It is interesting that in spite of a large number of energetically competing structures determined in theoretical calculations, experimental observations show the stability of only one classically oriented solid phase in a very broad pressure-temperature range [12,77]. The pressure and temperature dependencies of vibron and phonon frequencies suggest that phase III becomes more stable at higher pressures and lower temperatures. A rather strong softening of molecular vibron Raman mode (above 35 GPa) has been interpreted as a "harbinger" of molecular dissociation, but later it was understood (*e.g.*, Ref. 78) that a substantial part of this softening is coming from the increase of the intramolecular coupling [79,80]. The IR vibron, which contains much less contribution of this coupling starts softening only above 120 GPa [79]. However, unlike the situation with the classical soft modes related to the displacive phase transitions, there is no acceleration of the softening with pressure, making predictions of molecular dissociation with pressure rather uncertain [75]. Extrapolation of the optical data suggests that the optical closure in phase II should occur near 450 GPa [75,77]. The effect of temperature was recognized to be very essential for metallization of hydrogen in static high-pressure conditions [11,14].

6. Phase IV

Until 2011 only the high-pressure room-temperature studies of hydrogen up to 180 Gpa [10] and to the claimed 340 GPa have been reported 81,82. The latter results are very controversial mainly due to the fact that no positive diagnostics of hydrogen was offered. In Fig. 4 we show the compilation of the recently obtained Raman data on the molecular vibron up to 320 GPa compared to that reported previously by Ruoff [81]. The obvious conclusion is that either the pressure metrology in these early experiments was not reliable or other factors (*e.g.*, lack of hydrogen in the sample chamber) are responsible for apparent discrepancy with the current results. The diamond Raman edge is the currently adopted method of pressure measurements in ultra-high compression experiments. The Raman frequency of the diamond edge (*e.g.*, Ref. 15) has been calibrated with respect to other sensors (mostly ruby) and is reliable in situations when the experiments are performed in similar geometrical conditions. However the results of Ruoff [81] obviously stand alone (Fig. 4) making the claim of
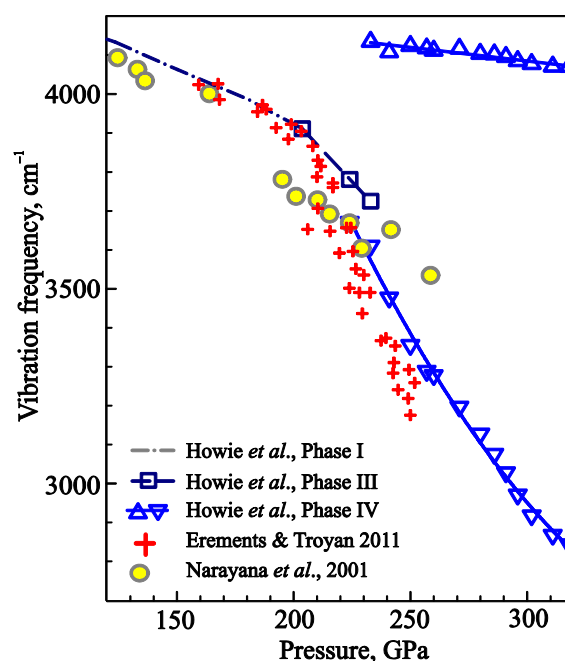

Fig. 4. (Color online) Raman vibron frequencies of hydrogen though the transition to phases III and IV at 300 K [10,11,14,81].

transparent hydrogen at 342 GPa in the subsequent paper [82], which also does not present any positive diagnostics of hydrogen, highly questionable.

Two independent experiments have recently succeeded in reaching pressures in excess of 300 GPa at 300 K [11,14]. Similar Raman observations have been reported that show remarkable changes in Raman spectra above 200 GPa; firstly: the gradient of the vibron frequency versus pressure slope changes dramatically and a broad low-frequency peaks appear, and secondly: another system of low-frequency high intensity peaks emerge and the vibron splits in two. Eremets and Troyan [14] did not notice the appearance of new low-frequency peaks and interpreted this change as due to a transition to the *Cmca*-12 phase [40]. They also reported a change in optical properties and a total disappearance of Raman signal above 260–270 GPa, which was suggested to be due to transformation to metallic monatomic fluid.

On the contrary, Howie *et al.* [11] observed Raman signal to the highest pressure reached in the experiment — 320 GPa. They noticed the appearance of a second Raman vibron with very different pressure behavior of both the frequency and linewidth. Based on these observations and theoretical predictions [40], they suggested a *Pbcn* structure for phase IV of hydrogen. This structure matches much better with the experimental observations, as the appearance of two distinct vibron modes and a strong low-frequency libron mode can be naturally explained based on the unique features of phase IV. Indeed, *Pbcn* hydrogen consists of molecular layers of two kinds: weakly bounded hexagonal, and strongly bounded graphene-like [40], which differ by the

intramolecular distances that are substantially larger in the graphene-like layer. It is interesting that the hexagonal configuration of molecules in the graphene-like layer is somewhat reminiscent to the prediction of LeSar and Herschbach (Ref. 83, see also Ref. 84), who suggested that termolecular complexes $[(H_2)_3]$ could form before the transition to the atomic phase. This structure has been further examined theoretically in a number of recent publications, which suggest slightly different crystal symmetries [13,85] and fluxional behavior of graphene-like layers [86] related to large atomic tunneling quantum effects, and even suggest quantum liquid behavior for these layers [87]. Experimental and theoretical studies clearly indicate that phase IV is insulating or semimetallic as the optical spectra show the presence of the optical gap [11,30].

7. Conclusions

Key questions still remain about the higher pressure behavior. Predictions propose that phase IV will transform to a metallic molecular phase with *Cmca*-4 structure above 360 GPa [86]. However, monatomic phases [88–90] may compete at these compressions. We believe that experimental static compression studies which will verify these predictions are down the road [91]. Such studies will also address the issue of the predicted ground state fluid atomic metallic hydrogen [92–94]. The central problem is the treatment of the quantum effects at such regimes, which needs to be solved for such fundamentally important system as the element number one.

Acknowledgment

1. W.J. Nellis, *Rep. Prog. Phys*. **69**, 1479 (2006).
2. A.F. Goncharov and R.J. Hemley, *Chem. Soc. Rev*. **35** (10), 899 (2006).
3. A.F. Goncharov and J. Crowhurst, *Phase Transitions* **80**, 1051 (2007).
4. E.G. Maksimov and Y.I. Shilov, *Usp. Fiz. Nauk.* **169**, 1223 (1999).
5. J.M. McMahon, M.A. Morales, C. Pierleoni, and D.M. Ceperley, *Rev. Mod. Phys*. **84**, 1607 (2012).
6. R. Jeanloz, P.M. Celliers, G.W. Collins, J.H. Eggert, K.K.M. Lee, R.S. McWilliams, S. Brygoo, and P. Loubeyre, *P. Natl. Acad. Sci. USA* **104**, 9172 (2007).
7. R.F. Trunin, V.D. Urlin, and A.B. Medvedev, *Phys. Usp*. **53** 577 (2010).
8. D.G. Hicks, T.R. Boehly, P.M. Celliers, J.H. Eggert, S.J. Moon, D.D. Meyerhofer, and G.W. Collins, *Phys. Rev. B*, **79**, 014112 (2009).
9. P. Loubeyre, S. Brygoo, J. Eggert, P.M. Celliers, D.K. Spaulding, J.R. Rygg, T.R. Boehly, G.W. Collins, and R. Jeanloz, *Phys. Rev. B* **86**, 144115 (2012).
10. B.J. Baer, M.E. Chang, and W.J. Evans, *J. Appl. Phys*. **104** (2008).
11. R.T. Howie, C.L. Guillaume, T. Scheler, A.F. Goncharov, and E. Gregoryanz, *Phys. Rev. Lett*. **108**, 125501 (2012).
12. C.S. Zha, Z.X. Liu, and R.J. Hemley, *Phys. Rev. Lett*. **108** 146402 (2012).
13. C.J. Pickard, M. Martinez-Canales, and R.J. Needs, *Phys. Rev. B* **85**, 214114 (2012).
14. M.I. Eremets and I.A. Troyan, *Nat. Mater.* **10**, 927 (2011).
15. Y. Akahama and H. Kawamura, *J. Appl. Phys.* **100**, 043516 (2006).
16. H.K. Mao and R.J. Hemley, *Rev. Mod. Phys*. 66, 671 (1994).
17. A.F. Goncharov, R.J. Hemley, and H.K. Mao, *J. Chem. Phys*. **134**, 174501 (2011).
18. I.I. Mazin, R.J. Hemley, A.F. Goncharov, M. Hanfland, and H.K. Mao, *Phys. Rev. Lett*. **78**, 1066 (1997).
19. A.F. Goncharov, I.I. Mazin, J.H. Eggert, R.J. Hemley, and H.K. Mao, *Phys. Rev. Lett*. **75**, 2514 (1995).
20. M.P. Surh, K.J. Runge, T.W. Barbee, E.L. Pollock, and C. Mailhiot, *Phys. Rev. B* **55**, 11330 (1997).
21. B.J. Baer, W.J. Evans, and C.S. Yoo, *Phys. Rev. Lett*. **98**, 235503 (2007).
22. B.J. Baer, W.J. Evans and C.S. Yoo, *Phys. Rev. Lett*. **102**, 235503 (2009).
23. P. Toledano, H. Katzke, A.F. Goncharov, and R.J. Hemley, *Phys. Rev. Lett*. **103**, 105301 (2009).
24. F. Datchi, P. Loubeyre, and R. LeToullec, *Phys. Rev. B* **61**, 6535 (2000).
25. E. Gregoryanz, A.F. Goncharov, K. Matsuishi, H. Mao and R.J. Hemley, *Phys. Rev. Lett*. **90**, 175701 (2003).
26. N. Subramanian, A.F. Goncharov, V.V. Struzhkin, M. Somayazulu, and R.J. Hemley, *P. Natl. Acad. Sci. USA* **108**, 6014 (2011).
27. S. Deemyad and I.F. Silvera, *Phys. Rev. Lett*. **100**, 155701 (2008).
28. M.I. Eremets and I.A. Trojan, *J. Lett*. **89**, 174 (2009).
29. S.A. Bonev, E. Schwegler, T. Ogitsu, and G. Galli, *Nature* **431**, 669 (2004).
30. R.T. Howie, T. Scheler, C.L. Guillaume, and E. Gregoryanz, *Phys. Rev. B* **86**, 214104 (2012).
31. I. Tamblyn and S.A. Bonev, *Phys. Rev. Lett*. **104**, 065702 (2010).
32. M.A. Morales, C. Pierleoni, E. Schwegler, and D.M. Ceperley, *P. Natl. Acad. Sci. USA* **107**, 12799 (2010).
33. L.J. Cui, N.H. Chen, and I.F. Silvera, *Phys. Rev. B* **51**, 14987 (1995).
34. I.F. Silvera and R.J. Wijngaarden, *Phys. Rev. Lett*. **47**, 39 (1981).
35. A.F. Goncharov, R.J. Hemley, H.K. Mao, and J.F. Shu, *Phys. Rev. Lett*. **80**, 101 (1998).
36. M. Hanfland, R.J. Hemley, and H.K. Mao, *Phys. Rev. Lett*. **70**, 3760 (1993).

37. A.F. Goncharov, J.H. Eggert, I.I. Mazin, R.J. Hemley, and H.K. Mao, *Phys. Rev. B* **54**, 15590 (1996).

38. H. Kitamura, S. Tsuneyuki, T. Ogitsu, and T. Miyake, *Nature* **404**, 259 (2000).

39. K.A. Johnson and N.W. Ashcroft, *Nature* **403**, 632 (2000).

40. C.J. Pickard and R.J. Needs, *Nat. Phys.* **3**, 473 (2007).

41. J.S. Tse and D.D. Klug, *Nature* **378**, 595 (1995).

42. Rodgers, *Solid State Commun.* **145**, 5 (2008).

43. J. Kohanoff, S. Scandolo, G.L. Chiarotti, and E. Tosatti, *Phys. Rev. Lett.* **78**, 2783 (1997).

44. J. Kohanoff, S. Scandolo, S. de Gironcoli, and E. Tosatti, *Phys. Rev. Lett.* **83**, 4097 (1999).

45. K.J. Runge, M.P. Surh, C. Mailhiot, and E.L. Pollock, *Phys. Rev. Lett.* **69**, 3527 (1992).

46. Y. Akahama, M. Nishimura, H. Kawamura, N. Hirao, Y. Ohishi, and K. Takemura, *Phys. Rev. B* **82**, 060101(R) (2010).

47. I. Goncharenko and P. Loubeyre, *Nature* **435**, 1206 (2005).

48. H. Kawamura, Y. Akahama, S. Umemoto, K. Takemura, Y. Ohishi, and O. Shimomura, *J. Phys.: Condens. Matter.* **14**, 10407 (2002).

49. X.-Z. Li, B. Walker, M.I.J. Probert, C.J. Pickard, R.J. Needs, and A. Michaelides, *J. Phys.: Condens. Matter.* **25**, 085402 (2013).

50. W.R. Magro, D.M. Ceperley, C. Pierleoni, and B. Bernu, *Phys. Rev. Lett.* **76**, 1240 (1996).

51. D. Saumon and G. Chabrier, *Phys. Rev. A* **46**, 2084 (1992).

52. S. Scandolo, *P. Natl. Acad. Sci. USA* **100**, 3051 (2003).

53. B. Boates and S.A. Bonev, *Phys. Rev. Lett.* **102**, 015701 (2009).

54. V. Diatschenko, C.W. Chu, D.H. Liebenberg, D.A. Young, M. Ross, and R.L. Mills, *Phys. Rev. B* **32**, 381 (1985).

55. A.F. Goncharov and J.C. Crowhurst, *Phys. Rev. Lett.* **96**, 055504 (2006).

56. S.T. Weir, A.C. Mitchell, and W.J. Nellis, *Phys. Rev. Lett.* **76**, 1860 (1996).

57. W.J. Nellis, S.T. Weir, and A.C. Mitchell, *Phys. Rev. B* **59**, 3434 (1999).

58. P. Loubeyre, P.M. Celliers, D.G. Hicks, E. Henry, A. Dewaele, J. Pasley, J. Eggert, M. Koenig, F. Occelli, K.M. Lee, R. Jeanloz, D. Neely, A. Benuzzi-Mounaix, D. Bradley, M. Bastea, S. Moon, and G.W. Collins, *High Pressure Res* **24**, 25 (2004).

59. P.M. Celliers, G.W. Collins, L.B. Da Silva, D.M. Gold, R. Cauble, R.J. Wallace, M.E. Foord, and B.A. Hammel, *Phys. Rev. Lett.* **84**, 5564 (2000).

60. A.F. Goncharov, D.A. Dalton, R.S. McWilliams, and M.F. Mahmood, *Mater. Res. Soc. Symp.DOI:10.1557/opl.2012.1560 (2012) Proc.* 1405 DOI:10.1557/opl.2012.1560 (2012).

61. I.F. Silvera, *Rev. Mod. Phys.* **52**, 393 (1980).

62. H.E. Lorenzana, I.F. Silvera, and K.A. Goettel, *Phys. Rev. Lett.* **64**, 1939 (1990).

63. F. Moshary, N.H. Chen, and I.F. Silvera, *Phys. Rev. Lett.* **71**, 3814 (1993).

64. H. Kawamura, Y. Akahama, S. Umemoto, K. Takemura, Y. Ohishi, and O. Shimomura, *Solid State Commun.* **119**, 29 (2001).

65. R.J. Hemley and H.K. Mao, *Phys. Rev. Lett.* **61**, 857 (1988).

66. L.J. Cui, N.H. Chen, and I.F. Silvera, *Phys. Rev. Lett.* **74**, 4011 (1995).

67. N.H. Chen, E. Sterer, and I.F. Silvera, *Phys. Rev. Lett.* **76**, 1663 (1996).

68. R.J. Hemley, I.I. Mazin, A.F. Goncharov, and H.K. Mao, *Europhys. Lett.* **37**, 403 (1997).

69. R.J. Hemley, Z.G. Soos, M. Hanfland, and H.K. Mao, *Nature* **369**, 384 (1994).

70. A.F. Goncharov, M.A. Strzhemechny, H.K. Mao, and R.J. Hemley, *Phys. Rev. B* **63**, 064304 (2001).

71. M. Plischke and B. Bergersen, in *Equilibrium Statistical Physics*, Prentice Hall, Englewood Cliffs, NJ, (1989), p. 74.

72. C.J. Pickard and R.J. Needs, *Phys. Rev. Lett.* **102** (2009).

73. E. Kaxiras and J. Broughton, *Europhys. Lett.* **17**, 151 (1992).

74. E. Kaxiras, J. Broughton, and R.J. Hemley, *Phys. Rev. Lett.* **67**, 1138 (1991).

75. A.F. Goncharov, E. Gregoryanz, R.J. Hemley, and H.K. Mao, *P. Natl. Acad. Sci. USA* **98**, 14234 (2001).

76. S. Azadi and T.D. Kuhne, *Pis'ma v ZhETF* **95**, 509 (2012).

77. P. Loubeyre, F. Occelli, and R. LeToullec, *Nature* **416**, 613 (2002).

78. N.W. Ashcroft, *Phys. Rev. B* **41**, 10963 (1990).

79. M. Hanfland, R.J. Hemley, H.K. Mao, and G.P. Williams, *Phys. Rev. Lett.* **69**, 1129 (1992).

80. F. Moshary, N.H. Chen, and I.F. Silvera, *Phys. Rev. B* **48**, 12613 (1993).

81. A.L. Ruoff, in: *High Pressure Science and Technology*, W. Trzeciakowski (ed.), World Scientific, Singapore, (1996).

82. C. Narayana, H. Luo, J. Orloff, and A.L. Ruoff, *Nature* **393**, 46 (1998).

83. R. Lesar and D.R. Herschbach, *J. Phys. Chem.* **85**, 3787 (1981).

84. V. Labet, R. Hoffmann, and N.W. Ashcroft, *J. Chem. Phys.* **136**, 074502 (2012).

85. H.Y. Liu, L. Zhu, W.W. Cui, and Y.M. Ma, *J. Chem. Phys.* **137**, 074501 (2012).

86. A.F. Goncharov, J.S. Tse, H. Wang, J.H. Yang, V.V. Struzhkin, R.T. Howie, and E. Gregoryanz, *Phys. Rev. B* **87**, 024101 (2013).

87. H. Liu and Y. Ma, *Phys. Rev. Lett.* **110**, 025903 (2013).

88. J.M. McMahon and D.M. Ceperley, *Phys. Rev. Lett.* **106**, 165302 (2011).

89. V. Labet, R. Hoffmann, and N.W. Ashcroft, *J. Chem. Phys.* **136**, 074504 (2012).

90. H.Y. Liu, H. Wang, and Y.M. Ma, *J. Phys. Chem. C* **116**, 9221 (2012).

91. L. Dubrovinsky, N. Dubrovinskaia, V.B. Prakapenka, and A.M. Abakumov, *Nat. Commun.* **3**, 1163 (2012).

92. E. Babaev, A. Sudbo, and N.W. Ashcroft, *Nature* **431**, 666 (2004).

93. E. Babaev, A. Sudbo, and N.W. Ashcroft, *Phys. Rev. Lett.* **95**, 105301 (2005).

94. J. Chen, X.-Z. Li, Q. Zhang, M.I.J. Probert, C.J. Pickard, R.J. Needs, A. Michaelides, and E. Wang, *arXiv:1212.4554v1* [*cond-mat.mtrl-sci*] (2012).